THE APPLICATION OF ELECTRON MICROSCOPY METHODS IN THE STUDY OF INVERSION BOUNDARIES IN ZnO-BASED VARISTORS

Nina Daneu, Aleksander Rečnik and Slavko Bernik
Jožef Stefan Institute, Ljubljana, Slovenia

TUTORIAL INVITED PAPER
MIDEM 2000 CONFERENCE – Workshop on ANALYTICAL METHODS IN MICROELECTRONICS AND ELECTRONIC MATERIALS
18.10.00- 20.10.00, Postojna, Slovenia

Keywords: ZnO varistors, Zinc Oxide varistors, ZnO ceramics, Zinc Oxide ceramics, IBs, Inversion Boundaries, electron microscopy methods, electronic microscopy, crystallography, SEM, Scanning Electron Microscopy, CTEM, Conventional Transmission Electron Microscopy, CBED, Convergent Beam Electron Diffraction, HRTEM, High-Resolution Transmission Electron Microscopy, HAADF-STEM, High-Angle Annular Dark Field Scanning Transmission Electron Microscopy, Z-contrast imaging, EDS, Energy Dispersive Spectroscopy

Abstract: Inversion boundaries in ZnO-based varistor ceramics were studied by various electron microscopy techniques. Scanning electron microscopy observations disclose a flat internal boundary in every ZnO grain. Etched cross-sections reveal the inversion of crystal domains over the fault plane. Microdiffraction experiments using a conventional transmission electron microscope proved that the faults are inversion boundaries, lying in basal planes of the hexagonal ZnO structure. The local structure was assessed by high-resolution transmission electron microscopy and chemistry of the fault was interrogated by energy dispersive spectroscopy. Regardless the type of the dopant (Sb, Sn, Ti, In, Fe, Ga, etc.) inversion boundaries possess a local cubic structure comprising a mixed close-packed cationic layer of octahedral coordination.

Uporaba metod elektronske mikroskopije za študij inverznih mej v varistorski keramiki na osnovi ZnO

Ključne besede: ZnO varistorji cink oksidni, ZnO keramika cink oksidna, IBs meje inverzne, metode spektroskopije elektronske, mikroskopija elektronska, kristalografija, SEM mikroskopija elektronska skanirna, CTEM mikroskopija elektronska konvencionalna, CBED difrakcija curka elektronskega konvergentnega, HRTEM mikroskopija elektronska z ločljivostjo visoko, HAADF-STEM mikroskopija elektronska skanirna s poljem temnim obročastim kota velikega, Z-kontrast upodabljanje, EDS spektroskopija z energijo razpršeno

Povzetek: Inverzne meje v varistorski keramiki na osnovi ZnO smo preiskovali z različnimi metodami elektronske mikroskopije. Opazovanje mikrostrukture na vrstičnem elektronskem mikroskopu pokaže ravno mejo v vsakem zrnu ZnO. Na inverzijo kristalnih domen preko ravnine defekta kaže že jedkana površina mikrostrukture. Z mikrodifrakcijskimi eksperimenti na konvencionalnem transmisijskem elektronskem mikroskopu smo dokazali, da so te napake inverzne meje in da ležijo v bazalnih ravninah heksagonalnega ZnO. Lokalno strukturo napak smo preiskali z visokoločljivostno transmisijsko elektronsko mikroskopijo, njihovo kemijsko sestavo pa smo analizirali z energijsko disperzijsko spektroskopijo. Ne glede na vrsto dopanta (Sb, Sn, Ti, In, Fe, Ga,) imajo inverzne meje lokalno kubično strukturo, ki se sestoji iz oktaederske plasti kationov.

1 Introduction

Inversion boundaries (IBs) play an important role in microstructure development /1/, as well as they are believed to affect the electrical properties /2/ of ZnO-based varistor ceramics. Inversion boundaries develop in ZnO grains only when ZnO is doped with specific metal oxides such as SnO_2 /1/, Sb_2O_3 /3-5/, TiO_2 /6/, In_2O_3 /7/, Fe_2O_3 /8/, Ga_2O_3 /9/, among others. The addition of SnO_2 to ZnO significantly influences the grain growth via the inversion boundary induced grain growth mechanism /1/. ZnO grains with IBs start to grow anisotropically along the direction of the fault plane until they collide. With the increasing amount of SnO_2 more ZnO grains initially contain IBs and the final grain size gets smaller. The most extensively studied system that exhibits IBs is certainly Sb_2O_3 doped ZnO because Sb_2O_3 is an essential dopant of varistor ceramics when fine-grained microstructure is required. It is believed that Sb_2O_3 influences the grain growth through the formation of secondary spinel grains and IBs in the ZnO grains. Final microstructures, obtained with the addition of small amounts of Sb_2O_3 are fine-grained and the final grain size gets even smaller with increasing addition of Sb_2O_3 /10/. Therefore, Sb_2O_3 is reported as an inhibitor of ZnO grain growth /11/. On the contrary, the addition of TiO_2 to ZnO ceramics results in a large final grain size and is typically added when coarse-grained microstructure is required. TiO_2 is believed to be a grain growth promoter /12/. Because of their influence to the final microstructure Sb_2O_3 is used in high-voltage, while TiO_2 is added for low-voltage varistor applications.

To understand the influence of these planar faults to ZnO grain growth we have to understand their nucleation mechanism and therefore the knowledge about their exact structural and chemical characterisation is required. In order to determine the local structure and chemistry of planar fault one should employ appropriate methods which enable its direct observation. To assess the information from sub-nanometer regions of the specimen we have to produce probes of that order of magnitude. Here electron microscopy provides a unique capability to retrieve a local structural informa-

Informacije MIDEM 30(2000)4, str. 228-232

tion that can not be recovered by statistical information obtained with X-ray crystallography. Apart from structural information, electrons and their energy dissipation products are bearing a valuable chemical information of the local structure owing to a wide variety of electronic transitions. In this paper the identification of inversion boundaries is given beginning with scanning electron microscope observations down to the detailed structural and chemical characterisation of these faults with the methods of analytical and phase contrast transmission electron microscopy.

2 Crystallography of inversion boundaries

ZnO crystallises in hexagonal wurtzite structure, in which the close-packed zinc and oxygen layers are exchanging in a ...αAβB... manner, where α and β are zinc, while A and B are oxygen atoms. Unit cell parameters are a=0,3253 nm and c=0,5213 nm /13/. Another parameter, typical for this structure is u, which is the atomic shift between oxygen and zinc atomic layers and amounts to 0.382 in hexagonal ZnO. Because of this, the structure does not poses a centre of symmetry in the direction of the c-axis, which is hence called the polar axis of the structure. According to the direction of the polar c-axis two basic types of planar faults can be distinguished in hexagonal ZnO: (a) stacking faults ...αA–βB | γC–βB..., where the direction of the polar axis over the fault is preserved and (b) inversion boundaries, where the direction of the polar axis is reversed across the fault plane. IBs can be of two configurations, head-to-head if the polar axes point toward the boundary or tail-to-tail if they point away from the boundary.

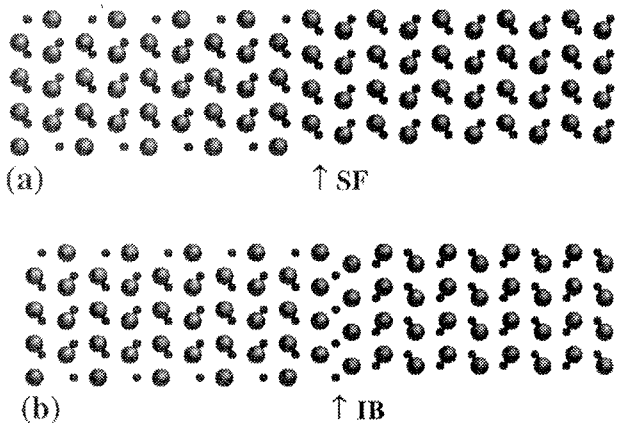

Fig. 1: Atomic structures of (a) stacking fault and (b) head-to-head inversion boundary.

Our recent studies of the crystallography of IBs in Sb_2O_3 doped ZnO indicate that the stacking across the fault plane is α_I A–β_IB–α_I A–β_IB |β_{oct}| Cγ_{II}–Bβ_{II}–Cγ_{II}–Bβ_{II} ... while the translation produced by such head-to-head IB is (1–2u)·[0001] + 1/3·[10$\bar{1}$0]. The IB plane itself comprises a close-packed layer of cations located at the octahedral interstices of this interface structure /14/.

The schematic drawings of basal plane stacking fault and head-to-head inversion boundary are illustrated in Figure 1.

3 Methods of investigation

Unlike the X-rays, lenses for electrons are readily made, allowing to produce electronprobes down to 0.2 nm in diameter. There are several reasons why electrons are more convenient as a probe for the studies of local structures in solids. They are strongly scattered by solids, allowing scattering and imaging experiments to be performed with a high information level. In general, structural information is obtained from elastically scattered electrons, whereas the information about the chemistry of the specimen is recovered from inelastically scattered electrons and electron decay products. In past few decades numerous methods exploiting different properties of electrons were developed, allowing the local structures of crystal defects to be studied.

The information about the structural and compositional properties of planar faults can be obtained employing a high-resolution transmission electron microscopy (HRTEM) combined with the energy dispersive X-ray spectroscopy (EDS) in the vicinity of the interface. Quantification of HRTEM and EDS data results in a detailed information about the orientation of the host crystal blocks, atomic-column positions along the interface in the selected projections, rough atomic-column displacements, chemical composition of the fault plane, and in some favourable cases also the oxidation state of the investigated atoms. It is important to note that non-periodic structural features, like point defects, happen to be beyond the capabilities of this approach.

3.1 Scanning electron microscopy (SEM)

Scanning electron microscopy is the most widely used tool for general microstructural characterisation of the samples. Depending on the detected electron signals, either topographic or chemical information can be obtained. Typically, for the grain size and morphology observations, the samples are etched thermally or chemically. Chemical etching with dilute hydrochloric acid results in dissolving of the intergranular material and therefore ZnO grains are easily observed. Additionally we observe that ZnO grains are etched differently depending on crystallographic orientation of the exposed surface. This phenomenon is characteristic also for other compounds having sphalerite or wurtzite structure /15/. Consequently planar faults, such as IBs become clearly visible after chemical etching. Another interesting feature produced by etching are the characteristic triangular etch pits on the surfaces of the ZnO grains. These etch-pits are always oriented in one direction in a single crystal domain. In ZnO grains contain planar faults the etch-figures always point towards the fault plane, and over the fault their orientation is reversed (Figure 2). These observations provide an indication, that the crystal orientation is reversed over the boundary, however the exact crystallographic plane of the fault can be assessed by a detailed investigations using transmission electron microscopy.

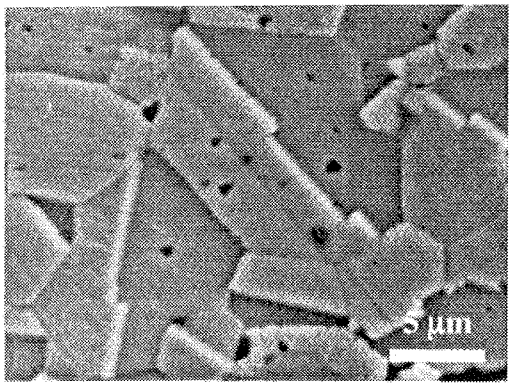

Fig. 2: SEM image of ZnO ceramics, doped with 0.1 mol% Sb_2O_3 and sintered at 1200°C for 16 hours. IBs intersecting ZnO grains are clearly visible. Triangular etch-pits in ZnO grains always point in the same direction within one crystal domain. In the grains with planar faults etch-pits always point towards the boundary, while over the fault their orientation is reversed, indicating the reversal of the polar c-axis.

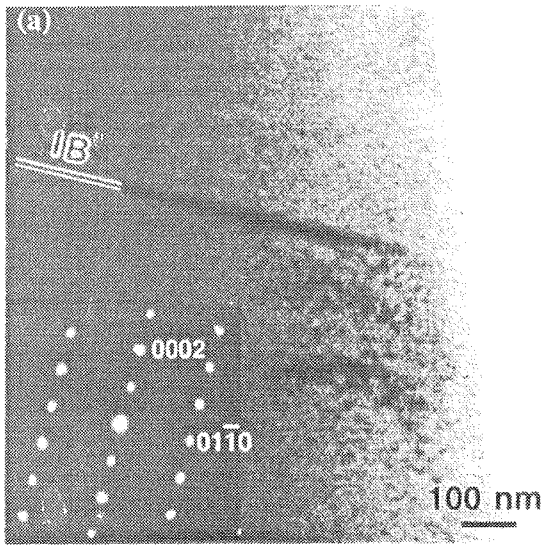

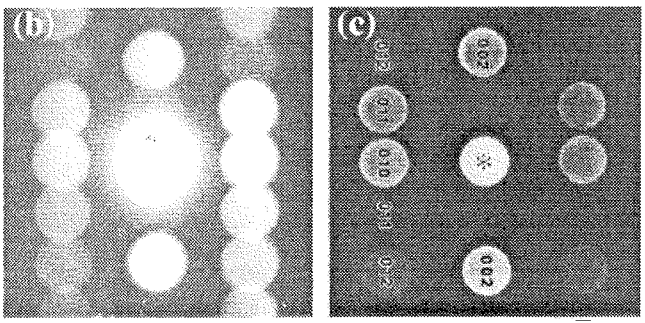

Fig. 3: (a) TEM image of a ZnO grain in the [11$\bar{2}$0] orientation, shows that the fault lies in the basal planes of the ZnO structure. Above are the (b) experimental and (c) simulated CBED patterns for the upper ZnO crystal domain while in the lower domain the pattern is mirrored (not shown here) indicating a head-to-head configuration of the inversion boundary.

3.2 Conventional transmission electron microscopy (CTEM)

Conventional transmission electron microscopy is the next step for identification and characterisation of the observed planar faults. TEM image in Figure 3 shows a planar fault intersecting the ZnO grain in the middle. According to the diffraction pattern, the fault lies in the basal planes of ZnO crystal. To determine the absolute orientation of the c-axis on both sides of the boundary we used a direct method, proposed by Mader and Rečnik /16/. Owing to non-centrosymmetric crystal structure, the scattering factors for **g** and **-g** reflections are different. The difference can be observed in a convergent beam electron diffraction (CBED) pattern, obtained with as small condenser aperture, that the diffraction disks do not overlap. Microdiffraction patterns on both sides of the boundary suggest a reversal of the polar c-axes. The absolute orientation of the crystal domains can be determined by matching the experimental microdiffraction patterns to calculated CBED patterns /17/ for a thin crystal regime.

3.3 High-resolution transmission electron microscopy (HRTEM)

In high-resolution transmission electron microscopy there are some instrumental and crystallographic limitations that have to be taken into account when choosing the appropriate zone axis for observation. The main obstacle is the resolution limit of the microscope and only in a few low-index crystallographic projections the fault can be aligned parallel to the electron beam. To study the basal plane IBs in ZnO this reduces the possibilities to [11$\bar{2}$0] and [10$\bar{1}$0] projections with a required resolution of 0.2817 nm in first and 0.1627 nm in the second instance. To obtain a 3D information about the local structure of the fault, and moreover to acquire the information on the atomic arrangement in the IB plane, lattice images in both projections were recorded under different defocusing conditions. Lattice images of IBs in Sb_2O_3 doped samples in the [11$\bar{2}$0] and [10$\bar{1}$0] projections have revealed the presence of heavy atoms in the boundary plane obeying an ...ABBABB... linear repeating sequence /14/. The translational state and coordination of the boundary plane could also be deduced from experimental HRTEM images. A lateral expansion of the IB observed in the lattice images allowed to differentiate this fault from stacking faults which are also abundant in ZnO /14/.

Our studies of IBs produced by doping ZnO with SnO_2 and In_2O_3 resulted in similar translation state across the fault plane and identical crystallography as determined for Sb_2O_3 doped samples. The only obvious difference was the linear repeating sequence in the boundary plane when viewed along the [10$\bar{1}$0] projection, which indicates that the distribution of dopant ions in the boundary plane is different for Sb_2O_3, SnO_2 and In_2O_3. While the linear repeating sequence for Sb-rich IB was ...ABBABB... /14/ this was in the case of Sn-rich IB ...AABBAABB... /16/ and ...AAA... /17/ for In-rich IB. Figure 4 shows typical lattice images of IBs viewed along the [10$\bar{1}$0] projection in SnO_2 and Sb_2O_3 doped ZnO. HRTEM results for different IBs show that the atomic arrangement of the IB octahedral plane and the

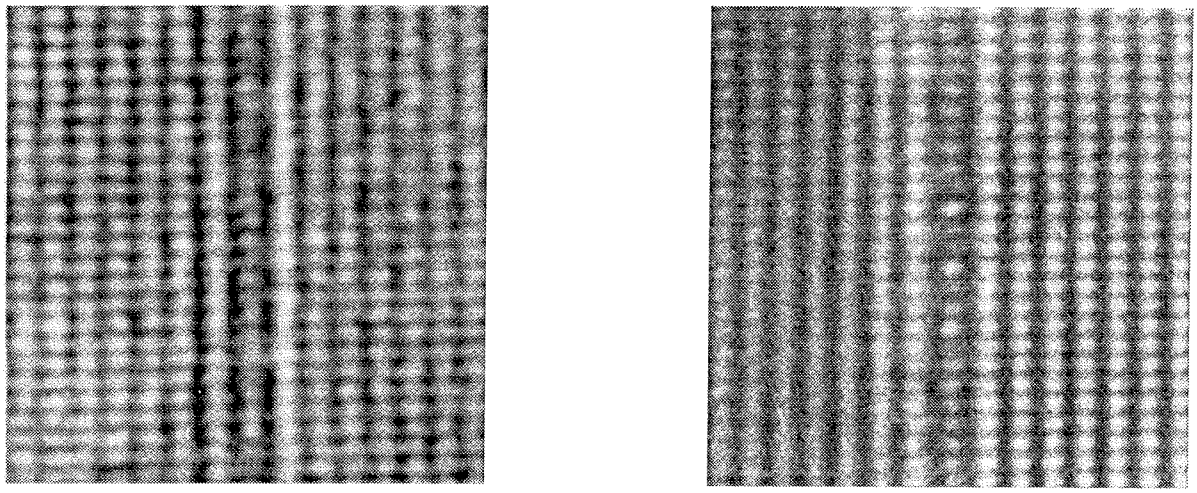

(a) (b)

Fig. 4: HRTEM images of IBs in (a) SnO_2 doped ZnO and (b) Sb_2O_3 doped ZnO in [10$\bar{1}$0] projection; note the periodicity of ...AABBAABB... and ...ABBABB... respectively.

amount of the dopant atoms mainly depend on the oxidation state of the dopant element. Therefore, to establish the content of the dopant in the fault plane one must obtain analytical information from IB.

3.4 Z-contrast scanning transmission electron microscopy (HAADF-STEM)

The correlation between the atomic structure and chemistry of solids became available by the atomic resolution high-angle annular dark field scanning transmission electron microscopy (HAADF-STEM), known as Z-contrast. The Z-contrast imaging can be performed using a field emission gun electron micro-scope equipped with a high-angle annular detector. HAADF-STEM in principle provides incoherent images that can be directly inverted to the object. While this is generally applicable for perfect crystal structures, image simulations are necessary for a quantitative elemental analysis /18/. To obtain the information on the local atomic arrangement in the IB octahedral plane we employed Z-contrast imaging of IBs in the [10$\bar{1}$0] zone axis. In the case of Sb-rich IBs we observed similar linear periodicity as from HRTEM images /19/. The intense white dots in the boundary plane produced by pure Sb columns are in the Z-contrast images separated by two dots of lower intensity, implying a boundary composition of $SbZn_2$.

3.5 Chemical analysis with energy dispersive spectroscopy (EDS)

HRTEM and Z-contrast imaging of IBs, formed with different dopants showed, that (a) inversion boundaries are single layers within the inverted ZnO crystal domains and (b) the phase contrast of different IBs is different. These observations indicate that IBs, formed with different dopants have different chemical composition and local structure. To quantitatively determine the chemical composition of different types of IBs one should employ energy dispersive spectroscopy (EDS), however, because of the very low dopant content (less than one monolayer) in the IB plane an appropriate method of exact dopant content in the boundary must be used. A single EDS analysis shows qualitatively that inversion boundaries formed with different dopants, contain only the IB forming element. To quantitatively determine the dopant level on IBs we used a method where dopant content in a boundary is estimated from a series of EDS analyses using different beam diameters. A series of EDS analyses on the IB plane with different beam diameters is performed, where the centre of the beam must be kept exactly the same in all measurements. From the dependency of the measured intensity ratio between the Zn–K_α line and a characteristic dopant line vs. the beam diameter, the integral amount of the dopant in the boundary layer can be calculated, assuming a straight boundary plane within a cylindrical volume of analysis /14/. Using this method we determined about 1/3 of a monolayer of Sb, 1/2 of a monolayer of Sn, and one full monolayer of In on inversion boundaries in ZnO doped with Sb_2O_3, SnO_2 and In_2O_3, respectively.

4 Summary

We have shown that a combination of various imaging and analytical techniques using scanning and transmission electron microscopy provides a powerful tool to study inversion boundaries in ZnO. The first evidence for the presence of inversion boundaries was given in SEM by observation of triangular etch-pits on both sides of planar faults intersecting the ZnO grains. The microdiffraction method performed in a CTEM on both sides of the boundary confirmed this presumption. To study the local structure and chemistry of IBs we used atomic resolution microscopy techniques. The structural information was obtained by studying the fault of interest in different zone axes by phase contrast HRTEM. The interpretation of experimental images is possible by the comparison with simulated ones. On the other hand the images obtained with HAADF-STEM method are incoherent and can be directly inverted to the object, which makes this technique a very promis-

ing tool for the studies where we need to correlate structure and chemistry of the fault. The combination of imaging methods combined with Z-contrast and EDS analysis of IBs showed, that different dopants form IBs with different local structure and chemistry.

References

/1/ N. Daneu, A. Rečnik, S. Bernik and D. Kolar, J. Am. Ceram. Soc., 83 (2000) 3165-71.

/2/ B. A. Haskell, S. J. Souri and M. A. Helfand, J. Am. Ceram. Soc., 82 (1999) 2106-10.

/3/ M. Trontelj and V. Kraševec, Science of Ceramics, 14 (1988) 915-920.

/4/ J. Bruley, U. Bremer and V. Kraševec, J. Am. Ceram. Soc., 75 (1992) 3127-28.

/5/ M. A. McCoy, R. W. Grimes and W. E. Lee, J. Mater. Res., 11 (1996) 2009-19.

/6/ D. Makovec and M. Trontelj, J. Am. Ceram. Soc., 77 (1994) 1202-8.

/7/ A. Loewe, M. Trontelj and W. Mader, Proceedings of the 1st Slovene-German Seminar on Joint Projects in Materials Science and Technology, Portorož, Slovenia, (1994) 35-40.

/8/ F. Wolf, A. Loewe and W. Mader, Abstracts of the 3rd Slovene-German Seminar on Joint Projects in Materials Science and Technology, Bled, Slovenia, (1998) 10-11.

/9/ J. Barf and W. Mader, Abstracts of the 3rd Slovene-German Seminar on Joint Projects in Materials Science and Technology, Bled, Slovenia, (1998) 86-87.

/10/ J. Kim, T. Kimura and T. Yamaguchi, J. Mater. Sci., 24 (1989) 2581-86.

/11/ T. Senda and R. C. Bradt, J. Am. Ceram. Soc., 74 (1991) 1296-1302.

/12/ D. Makovec, D. Kolar, and M. Trontelj, Mater. Res. Bull., 28 (1993) 803-11.

/13/ H. Schultz and K. H. Thiemann, Sol. State Commun., 32 (1979) 783-785.

/14/ A. Rečnik, N. Daneu, T. Walther and W. Mader, J. Mater. Res., to be published.

/15/ E. P. Warekois, M. C. Lavine, A. N. Mariano and H. C. Gatos, J. Appl. Phys., 33 (1961) 690-96.

/16/ W. Mader and A. Rečnik, Phys. Stat. Sol. (a), 166 (1998) 381-95.

/17/ P. A. Stadelmann, Ultramicroscopy, 21 (1987) 131-45.

/18/ T. Yamazaki, K. Watanabe, A. Rečnik, M. Čeh, M. Kawasaki and M. Shiojiri, J. Electron Microscopy, 49 (2000) in press.

/19/ A. Rečnik, W. Mader and M. Kawasaki, Proceedings of the 4th Multinational Congress on Electron Microscopy, Veszprém, Hungary, (1999) 113-118.

Nina Daneu
Aleksander Rečnik
Slavko Bernik
Jožef Stefan Institute
Jamova 39, 1000 Ljubljana, Slovenia
nina.daneu@ijs.si,
aleksander.recnik@ijs.si,
slavko.bernik@ijs.si

Prispelo (Arrived): 1.10.2000 *Sprejeto (Accepted): 25.11.2000*